Dielectric Normal Mode Process in Dilute Solutions of *cis*-Polyisoprene

Keiichiro Adachi* and Tadao Kotaka

Department of Macromolecular Science, Faculty of Science, Osaka University, Toyonaka, Osaka 560, Japan. *Received October 27, 1986*

ABSTRACT: Dielectric relaxation due to fluctuation of end-to-end distance of polymers termed the "normal mode process" was studied for dilute solutions of *cis*-polyisoprene having molecular weight, M, from 4×10^3 to 1×10^6 by using a good solvent, benzene, and a θ-solvent, dioxane. The observed relaxation times at finite concentrations, C, were converted to the relaxation times, τ_n°, at infinite dilution with the aid of Muthukumar's theory. The results were $\tau_n^\circ = 3.47 \times 10^{-15} M^{1.77}$ for benzene solutions at 298 K and $\tau_n^\circ = 1.26 \times 10^{-13} M^{1.49}$ for dioxane solutions at 308 K ($\simeq\theta$). The Zimm theory for the dielectric normal mode relaxation times was modified for the excluded volume effect by combining the observed intrinsic viscosity $[\eta]$ data with the theory. The result provided a satisfactory description of the M dependence of τ_n° for both benzene and dioxane (θ) solutions. The calculated values of the relaxation times, τ_1, for the first normal mode were in agreement with the benzene τ_n° data but were smaller than the dioxane data by a factor of 1.6. The shape of the loss curves reflecting the distribution of relaxation times was close to the theoretical curve given by the Zimm theory. From the dielectric relaxation strength, $\Delta\epsilon$, for the normal mode process, the mean square end-to-end distance, $\langle r^2 \rangle$, was calculated. For the benzene and dioxane solutions, $\langle r^2 \rangle$ was found to be proportional to $M^{1.2}$ and $M^{1.0}$, respectively.

Dielectric normal mode process due to fluctuation of end-to-end polarization has been a subject of long-lasting interest.[1-17] Recently, we found that *cis*-polyisoprene (*cis*-PI) has the component of the dipole moment parallel to the chain contour and reported the normal mode process of *cis*-PI in undiluted state[10,12] and concentrated solutions.[13]

Experimental studies on the normal mode process in dilute solutions have been reported by only a few authors for polymers having a rather limited range of molecular weights, M.[7-9] Jones et al.[7] studied solutions of poly(ϵ-caprolactone) with M ranging from 30×10^3 to 100×10^3 and observed the normal mode process in the frequency region of ca. 10 kHz. Mashimo et al.[8] used benzene solutions of low M poly(propylene oxide) with $M \simeq 2000$–4000 and found the loss maximum due to the normal mode at about 1 MHz. Previously, we also reported the normal mode process in solutions of poly(dichloro-1,4-phenylene oxide) having long chain branchings.[9] In these studies, the agreement between the observed relaxation time, τ_n, and the theoretical longest relaxation time, τ_1, given by the Rouse–Zimm theory[18,19] was confirmed. However, the M dependence of τ_n has not been fully investigated.

To compare the M dependence of τ_n with the Rouse–Zimm theory, it is desirable to determine τ_n at infinite dilution. In the previous studies,[7-9] solutions of 3–5% concentrations were used. Among these studies, only Jones et al.[7] extrapolated the relaxation frequency, ω, to zero concentration and compared ω at zero frequency with the theoretical values predicted by the free-draining[18] and nondraining[19] models. In the present study, we used solutions of well-characterized *cis*-PI having M from 4×10^3 to 1×10^6 with the concentration, C, as low as 0.4% to minimize the concentration effect. The observed relaxation times were converted to the values at infinite dilution by using the theory of Muthukumar and Freed.[20,21]

As reported previously, we determined the mean square end-to-end distance, $\langle r^2 \rangle$, from the dielectric relaxation strength, $\Delta\epsilon$, for the normal mode process.[13] Usually, we calculate dipole moments using the internal fields proposed by Lorentz or by Onsager.[22] However, in the case of the normal mode process, we found that the ratio of the internal to external field is close to unity, being independent of the solvent polarity. On the basis of this result, we examined the M dependence of $\langle r^2 \rangle$ in dilute solutions of *cis*-PI dissolved in a good solvent, benzene, and a θ-solvent, dioxane.

Table I
Characteristics of *cis*-Polyisoprene Samples

code	$10^{-3}M_w$	M_w/M_n	code	$10^{-3}M_w$	M_w/M_n
PI-74	74	1.18	PI-394	394	1.22
PI-164	164	1.17	PI-1250	1250	1.57
PI-272	272	1.29			

Experimental Section

Samples of *cis*-PI were prepared by anionic polymerization with *n*-butyllithium in *n*-pentane at about 20 °C. The absolute value of weight average molecular weight, M_w, was determined by low-angle light scattering, and the M_w/M_n ratio was calculated from the gel permeation chromatogram. The samples reported previously were also used.[12] Unfortunately, the samples with $M > 3 \times 10^5$ had a broad distribution of molecular weight. Thus, we fractionated the high molecular weight samples using benzene and methanol. The characteristics of the newly prepared samples are shown in Table I, in which the number in the sample code indicates the weight average molecular weight, M_w, in the unit of 10^3. The solvents, benzene (Bz) and dioxane (Diox), were purified by vacuum distillation with calcium hydride.

Since dioxane is hygroscopic, special care was taken to prepare sample solutions: Firstly, a definite amount of *cis*-PI was taken in a glass ampule and dried under vacuum of 10^{-2} Pa by joining the ampule to a vacuum line. Secondly, the purified dioxane was transferred by vacuum distillation to the ampule, which was, in turn, sealed and kept until the solution became homogeneous. Concentration was determined by weighing the whole glass ampule. Subsequently, the sample solutions were handled under atmosphere of dry nitrogen to avoid the moisture.

Concentrations of solutions were adjusted to be 0.3–0.5 wt % for *cis*-PI with $M > 1.64 \times 10^5$. However, for low M *cis*-PI, the concentration was 1–5%, because the low M *cis*-PI showed dispersion in the range 10^5–10^7 Hz, in which the sensitivity of the bridge was low.

Dielectric measurements were carried out from 3 Hz to 100 MHz with a transformer bridge (General Radio 1615 A) and a twin T-type bridge (Fujisoku DLB 1101D). The cell was the same type as reported previously.[13] However, since the dipole moment of *cis*-PI solutions is small, the dielectric measurements were made by using a cell with the relatively large empty capacitance of ca. 100 pF. We estimate the error in ϵ'' measurement to be less than 3% in the frequency range from 200 Hz to 20 kHz, but in the range below 100 Hz and above 100 kHz, the error is ca. 5%. The reliable ϵ' data was obtained only in the range below 50 kHz.

0024-9297/87/2220-2018$01.50/0

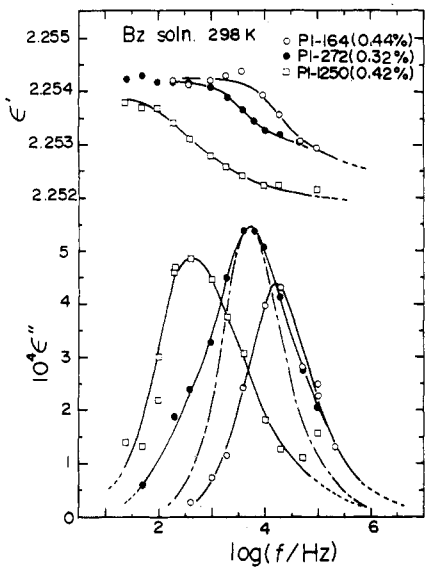

Figure 1. Dielectric constant ϵ' and loss factor ϵ'' at 298 K for dilute solutions of PI-164, PI-272, and PI-1250 dissolved in benzene. Solid lines are for guiding the eye. Dash-dot line represents the theoretical loss curve given by the Zimm theory (eq 1). Concentration is given in this figure in g cm^{-3}.

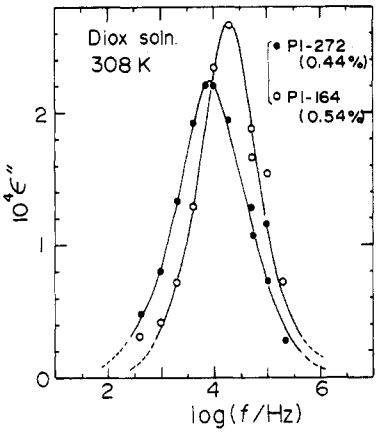

Figure 2. Dielectric loss factor ϵ'' at 308 K (θ) for dioxane solutions of PI-164 and PI-272. Solid lines are drawn to guide the eye. Concentration is given in g cm^{-3}.

Results and Discussion

Dielectric Dispersion in Solutions. Dielectric measurements were carried out at 298 K for benzene solutions and at 308 K for dioxane solutions. The θ-temperature of *cis*-PI/Diox system was reported to be 307 K.[23] Figures 1 and 2 show some typical dispersion curves for benzene and dioxane solutions of high M *cis*-PI, respectively.

As is seen, the frequency, f_m, of the loss maximum shifts to the lower frequency side with increasing M. This behavior is characteristic of the normal mode process. By comparing Figures 1 and 2, we notice that in the dioxane solutions the magnitude of the ϵ'' curve is about half of the benzene solutions. This indicates that the relaxation strength and, hence, $\langle r^2 \rangle$ in dioxane are lower than that in benzene.

The dash-dot line in Figure 1 shows the ϵ'' curve given by the Zimm theory[19]

$$\epsilon'' = (8\Delta\epsilon/\pi^2)\sum\omega\tau_p/[p^2(1 + \omega^2\tau_p^2)] \quad (p: \text{ odd}) \quad (1)$$

where $\Delta\epsilon$ is the relaxation strength; p, the number of the normal mode; and τ_p, the dielectric relaxation time for the pth normal mode which is twice the pth mechanical relaxation time. The shape of the observed ϵ'' curve is almost the same as the theoretical curve, as discussed later.

Table II
Dielectric Relaxation Times (τ_n),[a] Concentration (C), Relaxation Time (τ_n°) at Infinite Dilution, and Δ = log (τ_n/τ_n°)

code	10^2C	log τ_n	Δ	log τ_n°
		Benzene Solutions		
PI-05	5.60	−7.80	0.05	−7.85
PI-09	4.50	−7.25	0.06	−7.31
PI-11	5.14	−7.42	0.09	−7.51
PI-16	5.20	−7.10	0.13	−7.23
PI-42	2.50	−6.05	0.13	−6.18
PI-102	0.74	−5.54	0.07	−5.61
PI-164	0.44	−5.03	0.06	−5.09
PI-272	0.324	−4.55	0.07	−4.62
PI-394	0.336	−4.36	0.10	−4.46
PI-1250	0.418	−3.45	0.41	−3.86
		Dioxane Solutions		
PI-09	5.70	−7.0[b]	0.05	−7.05
PI-74	0.673	−5.45	0.06	−5.51
PI-102	0.677	−5.45	0.07	−5.52
PI-164	0.537	−5.12	0.06	−5.18
PI-272	0.444	−4.70	0.07	−4.77
PI-394	0.423	−4.55	0.08	−4.63

[a] Units of τ and C are s and g cm^{-3}, respectively. [b] Experimental error is ca. ±0.1.

Relaxation Time at Infinite Dilution. The dielectric relaxation time, τ_n, for the normal mode process was determined from the loss maximum frequency, f_m, with the relation $\tau_n = 1/(2\pi f_m)$. As pointed out by Jones et al.,[7] the value of τ_n thus determined for the theoretical ϵ'' curve constructed from the Rouse–Zimm theory is only 5% shorter than the theoretical longest relaxation time, τ_1, of the model. Thus, we used τ_m to evaluate the relaxation time τ_n° at infinite dilution for comparison with τ_1. The results were listed in Table II together with the concentration, C, in g cm^{-3}.

To discuss the M dependence of the relaxation time, τ_n°, at infinite dilution, it is necessary to reduce the observed τ_n to τ_n°. Muthukumar[20] expressed the C dependence of the relaxation time, τ_p, for the pth normal mode as

$$\tau_p = \tau_p^\circ[1 + CAp^{-\kappa} - 2^{0.5}(CAp^{-\kappa})^{1.5} + 2(CAp^{-\kappa})^2] \quad (2)$$

where A is a constant depending on M and κ is another parameter depending on the solvent quality. According to Muthukumar and Freed,[21] A is proportional to $M^{3\nu-1}$. Here, ν is the Flory constant characterizing the M dependence of $\langle r^2 \rangle^{0.5}$. For benzene and dioxane solutions of *cis*-PI, ν is taken to be $^3/_5$ and $^1/_2$, respectively. The exponent κ is equal to $3\nu - 1$ and corresponds to the exponent of the Mark–Houwink–Sakurada equation.

In order to reduce τ_n to τ_n°, we first determined the values of A for the benzene and dioxane solutions of PI-164 and PI-09. Figure 3 shows the C dependence of the experimental values of τ_n and the theoretical τ_1 given by eq 2 (with p = 1) for these solutions. The best fit of the theory was obtained by putting A = 47, 41, and 8.0 for PI-164/Bz, PI-164/Diox, and PI-09/Bz systems, respectively. These values are similar in magnitude to those reported for polystyrene in benzene.[24] Using these values and the theoretical M dependence of A, we approximated A as

$$A(M) = 3.16 \times 10^{-3}M^{4/5} \quad \text{(for Bz solutions at 298 K)} \quad (3)$$

$$A(M) = 1.01 \times 10^{-1}M^{1/2} \quad \text{(for Diox solutions at 308 K } (\theta)) \quad (4)$$

Using eq 2–4, we calculated the correction factor Δ = log

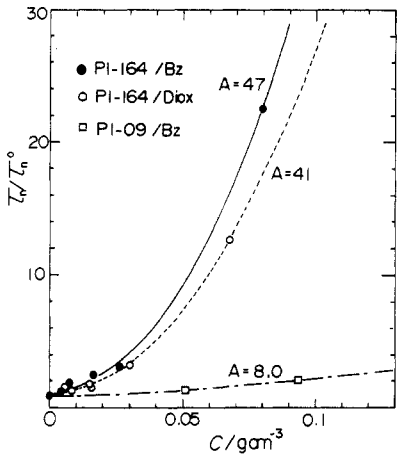

Figure 3. Concentration dependence of $\tau_n(C)/\tau_n^\circ$ for PI-164/Bz, PI-164/Diox, and PI-09/Bz systems. Here, $\tau_n(C)$ and τ_n° denote the relaxation time for the normal mode process at concentration, C, and at infinite dilution, respectively. Solid, dotted, and dash-dot lines show the Muthukumar theory[20] given by eq 2. Corresponding parameters are given in the figure.

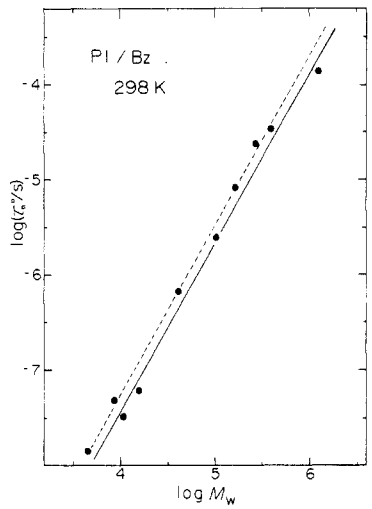

Figure 4. Molecular weight dependence of the relaxation time at infinite dilution for benzene solutions of *cis*-PI at 298 K. The solid and dashed lines show the theoretical relaxation times given by the nondraining model, eq 9, and by the free-draining model, eq 10, respectively.

(τ_1/τ_1°) appropriate to each solution for reducing τ_n to τ_n°. In the calculation, p was assumed to be 1 since usually only the first normal mode was always dominant. The results are listed in Table II and plotted in Figures 4 and 5. From the least-squares fitting of the τ_n° data, these results may be summarized as

$$\tau_n^\circ = 3.47 \times 10^{-15} M^{1.774} \text{ (for Bz at 298 K)} \quad (5)$$

$$\tau_n^\circ = 1.26 \times 10^{-13} M^{1.488} \text{ (for Diox at 308 K } (\theta)) \quad (6)$$

According to Zimm,[19] τ_p for the nondraining model is given by

$$\tau_p = \pi^{3/2}\eta_s\sigma^3 N^{3/2}/(12^{1/2}k_B T\lambda_p) \quad (7)$$

where σ is the average distance between beads; N, the number of beads; η_s, the solvent viscosity; and λ_p, the pth eigenvalue. On the other hand, according to Rouse, τ_p for the free-draining model is written as[18,25]

$$\tau_p = f_0\sigma^2 N^2/(3\pi^2 k_B T p^2) \quad (8)$$

where f_0 is the friction constant of the bead. Thus, the Zimm model predicts the $M^{1.5}$ dependence of τ_1, but the Rouse model predicts the M^2 dependence.

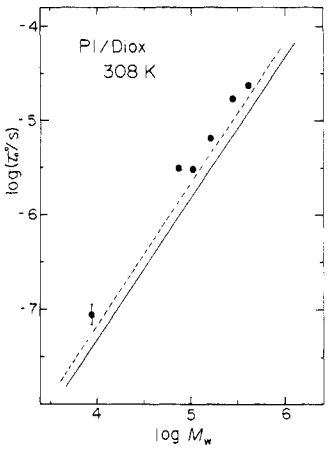

Figure 5. Relaxation time at infinite dilution for dioxane solutions of *cis*-PI at 308 K (the θ-state). The solid and dashed lines show the nondraining and free-draining models, respectively.

Comparing eq 5 and 6 with τ_1 given by eq 7 and 8, we notice that the Zimm theory predicts, at least, the correct $M^{1.5}$ dependence of the dioxane data, while neither the Rouse nor the Zimm theory predicts the $M^{1.77}$ dependence of the benzene data. This is not surprising because the excluded volume effect is not taken into account in both the Zimm and Rouse theories. However, the excluded volume effect may be incorporated in an ad hoc manner, as often done,[1-9] by combining the expression of intrinsic viscosity $[\eta]$ of the models with eq 7 or 8. The results read

$$\tau_p = 2M\eta_s[\eta]/(0.586RT\lambda_p) \quad (9)$$

for the Zimm (non-free-draining) model and

$$\tau_p = 12M\eta_s[\eta]/(\pi^2 RTp^2) \quad (10)$$

for the Rouse (free-draining) model. Since $[\eta] \propto M^\alpha$, both theories predict the relaxation time, τ_1, proportional to $M^{1+\alpha}$ with a small difference in the numerical front factor. Thus, instead of the theoretical prediction of $[\eta]$, we use the experimental values of $[\eta]$ in eq 9 and 10 to calculate τ_1. For benzene and dioxane, the solvent viscosities, η_s, were reported to be 0.603×10^{-2} at 298 K and 1.00×10^{-2} P at 308 K, respectively,[26] and the Mark–Houwink–Sakurada equations for *cis*-PI reported by Poddubnyi and Ehrenberg[23] were $[\eta] \propto M^{0.78}$ in benzene and $[\eta] \propto M^{0.5}$ in dioxane. Using these values, we obtain from eq 9 and 10 the full and dashed lines, respectively, for the Zimm and Rouse models, such as shown in Figures 4 and 5.

In these figures, we notice that experimental τ_n° for benzene solutions is rather close to the semiempirical theory, while those for dioxane solutions are larger than the theoretical τ_1 values by a factor of about 1.6. These results are rather strange because the bead-spring model assumes no excluded volume effect, and hence we expect that the τ_n° data in a θ-solvent should agree better with the theory than those in a good solvent. In fact, the Zimm theory predicted, at least, the correct M dependence of the dioxane data, and the Rouse and Zimm theory explain the M dependence of τ_n° over a wide range of M, when we introduce $[\eta]$ data. However, as far as the absolute maganitude of τ_1 is concerned, the disagreement of the theory with the dioxane data is opposite to this expectation.

Shape of the Loss Curves. Now, we turn our attention to the problem of the shape of the loss curves. As given by eq 1, there exist higher order modes causing the ϵ'' curve to be broader than an ϵ'' curve with a single relaxation time (the Debye dispersion curve).

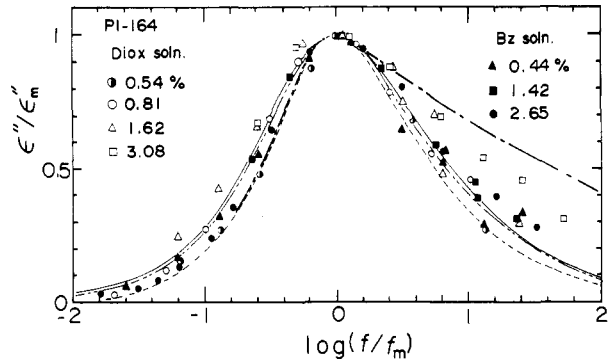

Figure 6. Comparison of the shape of the loss curve for solutions of PI-164. Concentration is given in unit of g cm^{-3}. Solid line and dash-dot-dot line show theoretical ϵ'' curves calculated by taking into account the distribution of molecular weight (see text) for benzene and dioxane solutions. Dashed and dash-dot lines show the loss curve given by the Zimm theory[19] and that calculated from the autocorrelation function reported by Verdier.[30]

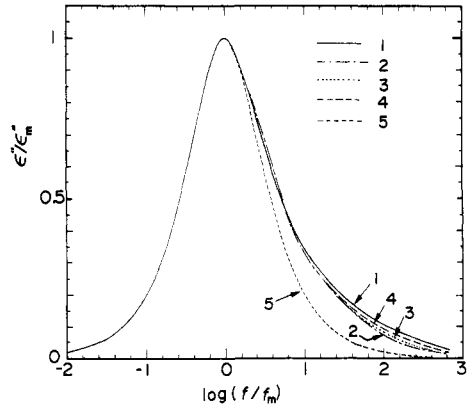

Figure 7. Theoretical dielectric loss curves. Curve 1, free-draining model (eq 1 and 8). Curve 2, nondraining model (eq 1 and 9). Curve 3, Tschoegl theory[27] with excluded volume effect with ϵ = 0.2. Curve 4, the ϵ'' curve for the benzene solution of PI-164 with C = 0.02 (eq 12). Curve 5, Debye single dispersion curve.

Figure 6 shows the ϵ''/ϵ''_m vs. log (f/f_m) plots for benzene and dioxane solutions of PI-164. Here ϵ''_m denotes the maximum value of ϵ''. The curve shown by the dashed line shows the theoretical ϵ'' curve calculated by the nondraining model of the Zimm theory. Experimental loss curves are broader than the theoretical one.

The shape of the loss curve is affected by several factors: hydrodynamic interactions,[18,19] excluded volume effect,[27,28] concentration,[20,21] and distribution of molecular weight. Among these factors, the distribution of molecular weight may be taken care of, if the molecular weight distribution of the particular sample is known and if an adequate ϵ'' curve may be assigned for the monodisperse sample. In the following, we review briefly the theories to describe the influences of these factors on the higher order terms.

A comparison of the ϵ'' curve given by the free-draining[18] and nondraining[19] models is shown in Figure 7. As long as we use eq 9 or 10 for τ_p, the difference in the shape of the ϵ'' curve due to hydrodynamic interaction is small in the range of frequency of ±2 decades from the loss maximum frequency, f_m. It is known that the complex shear moduli, $G^*(\omega)$, calculated by the free-draining and nondraining models show an appreciable difference in the high-frequency region.[25] This is in contrast to the result shown in Figure 7. In the mechanical relaxation, every pth mode contributes equally to $G^*(\omega)$ by a factor of CRT/M, while in the dielectric relaxation the weight of the pth mode is proportional to $1/p^2$. Thus, the ϵ'' curve is less sensitive to the higher order terms than the $G^*(\omega)$ curve.

Tschoegl[27] solved the eigenvalue equation for solutions in a good solvent based on the theory of Ptisyn and Eizner.[28] The hydrodynamic interaction parameter, h, is given by

$$h = 2^{\epsilon/2}Nf_o/[(12\pi^3)^{1/2}\eta_s\sigma N^{(1+\epsilon)/2}] \quad (11)$$

where $\epsilon = \nu - 1$ and other symbols are defined in eq 7–10. Using eq 11a–14 of ref 27, we evaluated the eigenvalues λ_p^* for ϵ = 0.2 and h = 100. The ratio of τ_1/τ_p which is equal to λ_p^*/λ_1^* is calculated to be 6.46, 14.93, 25.79, 38.78, and 53.6, respectively, for p = 3, 5, 7, 9, and 11. These ratios are only slightly larger than those calculated by Zimm et al.[29] without introducing the excluded volume effect. The ratio λ_p^*/λ_1^* for h = 30 and 300 was almost the same as the value at h = 100 within the difference of less than 0.5%. As shown in Figure 7, the theoretical loss curve calculated in this way is very close to the loss curve calculated by the Zimm theory.

Verdier[30] calculated the autocorrelation function, $\langle r(0)r(t)\rangle$, of the end-to-end vector by computer simulation. He used self-avoiding random walk on a simple cubic lattice and demonstrated that the distribution of the relaxation times increased as the number, N, of the steps was increased. Recently, similar calculation was also reported by Kovac et al.,[31] who showed that τ_p with the excluded volume effect was proportional to $p^{-2.14}$. In order to compare the results obtained by Verdier with our experimental results, we transformed $\langle r(0)r(t)\rangle$ to the ϵ'' curve for N = 64. As shown in Figure 6, Verdier's result gives a much broader ϵ'' curve compared with the one predicted by the Zimm theory.

As to the effect of concentration, eq 2 predicts that τ_1/τ_p for the case of $CA \ll 1$ is given by

$$\tau_1/\tau_p \simeq (\tau_1^o/\tau_p^o)[1 + CA(1 - p^{-\kappa})] \quad (12)$$

where κ is 0.5 in a θ-solvent and 0.65∼0.8 in a good solvent.[20,21] For solutions of PI-164, we determined A to be 47 and 41 in benzene and dioxane, respectively. Using these values and eq 12, we calculated the ϵ'' curve for C = 0.01 and 0.02. For τ_p^o, we used the Zimm theory at the nondraining limit. In Figure 7, the ϵ'' curve for C = 0.02 is shown. We can conclude that effect of concentration on the shape of the ϵ'' curve is very small in the range C < 0.02.

Now we turn to our experimental results shown in Figure 6. First we compare the shape of the ϵ'' curves of benzene and dioxane solutions. Though the data points are scattered, we notice that at 0.5–0.8% concentration, the ϵ'' curve for the dioxane solution is only slightly narrower than that of the benzene solution. Similar trend was also seen in the solutions of *cis*-PI with different M. As seen in Figure 6, the experimental loss curve for benzene solution did not show such a strong excluded volume effect as demonstrated by Verdier by computer simulation.[30] Accordingly, we conclude that the effect of the excluded volume effect is small as predicted by Tschoegl.[27]

In Figure 6, we see that with increasing concentration up to 1.5–3%, the width of the ϵ'' curve for the dioxane solutions became broad somewhat faster than that for the benzene solutions. The ϵ'' curves of the dioxane solutions appear to be sensitive to the change in C than those of the benzene solutions. However, this trend is opposite to the prediction of eq 12, which indicates that τ_1/τ_p for solutions in a good solvent becomes larger than that in a θ-solvent.

As pointed out above, the observed ϵ'' curves are broader than any of the theoretical loss curves except the simulated curve based on Verdier's self-avoiding random walk. This may be attributed to the influences of the distribution of molecular weight. To check this, we calculated an ϵ'' curve

for PI-164 by using the molecular weight distribution function, $\psi(M)$, determined by gel permeation chromatography

$$\epsilon''(\omega) = \int \psi(M)\epsilon''_z(M,\omega)\, d \ln M \qquad (13)$$

where $\epsilon''_z(M,\omega)$ denotes the theoretical ϵ'' curve given by the nondraining model and eq 9 was used for the M dependence of τ_p. As shown in Figure 6, the ϵ'' curve thus calculated coincides fairly well with the observed ϵ'' curves for the solutions of $C \simeq 0.005$. Therefore, we may conclude that broadening of the loss curves is mainly due to the distribution of molecular weight.

We recognize in Figure 1 that the ϵ'' curve for PI–1250 is broader than those of other low M samples such as PI-272 and PI-164. If this trend is due to the excluded volume effect, the trend is in agreement with the result deduced from Verdier's autocorrelation function. However, as shown by the dash-dot line in Figure 6, the ϵ'' curves calculated from the Verdier's model with $N = 64$ appear to be too broad as compared with the ϵ'' curves for the benzene solutions. Thus, the broader ϵ'' curve of PI-1250 may be again attributed to the distribution of molecular weight.

Relaxation Strength. The dielectric relaxation strength, $\Delta\epsilon$, for the normal mode process is given by

$$\Delta\epsilon/C = 4\pi N_A \mu^2 \langle r^2 \rangle F/(3k_B TM) \qquad (14)$$

where C is the concentration in unit of polymer weight per unit volume (density in case of the bulk state); N_A, Avogadro's constant; μ, the dipole moment per unit contour length; and F, the ratio of the strength of the internal to external electric field. Previously, we showed that F for the normal mode process is close to unity.[13] Thus, we expect that $\Delta\epsilon/C$ is independent of M in a θ-solvent and is proportional to $M^{1/5}$ in a good solvent.

To test this relationship, we determined $\Delta\epsilon$ from the area under the ϵ'' curve. To this end, we extrapolated the tails of the ϵ'' curve in the high- and low-frequency region, as shown by the dashed lines in Figures 1 and 2. We estimated the error due to this ambiguity in determination of $\Delta\epsilon$ to be ±20%. For some limited solutions in which relaxation region is below 10 kHz, the ϵ' data were available. We also determined $\Delta\epsilon$ from Cole–Cole plot for these solutions and found that the value thus determined was similar to that from the area of the loss curve. We used these data without extrapolating to zero concentration. The concentration for each solution is given in Table I.

Figure 8 shows the double logarithmic plot of $\Delta\epsilon/C$ vs. M. Previously, we estimated μ from the relaxation strength, $\Delta\epsilon$, for undiluted *cis*-PI to be 4.80×10^{-12} esu using $\langle r^2 \rangle$ determined from $[\eta]$ for dioxane solutions of *cis*-PI at the θ-temperature.[12] Using this value, we converted $\Delta\epsilon/C$ of the present study to $\langle r^2 \rangle/M$ as shown in Figure 8. The absolute value of $\langle r^2 \rangle/M$ thus determined depends on the accuracy of $[\eta]$. However, the relative $\langle r^2 \rangle$ values of the solutions can be determined only by the dielectric data. It is also noted that the dielectric constants of benzene and dioxane are 2.26 and 2.19, respectively, and therefore the ratio of the strength of F in benzene and dioxane solutions is very close to unity even if the Lorentz field is valid.

It is seen that $\Delta\epsilon/C$ in benzene solutions is higher than that in dioxane solution and increases with M. The slope of the solid line in the figure is 0.20, which is expected from the Flory theory. On the other hand, the dashed line and dot-dashed lines show $6\langle s^2 \rangle/M$ calculated by using the Flory–Fox equation[32] with $\Phi = 2.1 \times 10^{21}$ and 1.7×10^{21} dL/g, respectively, from the $[\eta]$ data of Poddubnyi and Ehrenberg for the benzene solutios of *cis*-PI.[23] The latter

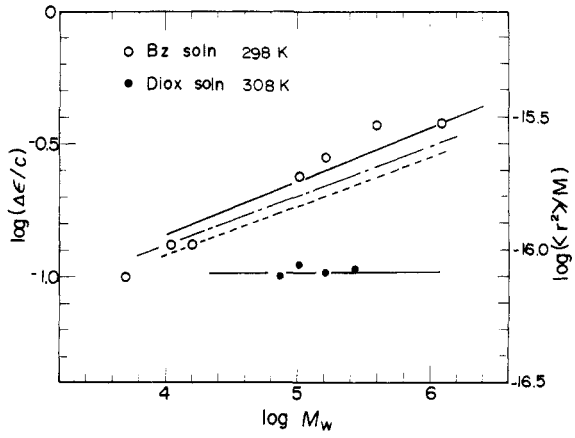

Figure 8. Molecular weight dependence of the reduced relaxation strength $\Delta\epsilon/C$ and $\langle r^2 \rangle/M$ for dilute solutions of *cis*-polyisoprene in benzene (good) and dioxane (θ). Upper solid line shows the slope = 0.2. Dashed line and dash-dot line show $6\langle s^2 \rangle/M$ calculated by the Flory–Fox[32] equation with $\Phi = 2.1 \times 10^{21}$ and 1.7×10^{21} dL g^{-1}, respectively. Here $\langle s^2 \rangle$ is the mean square radius of gyration.

value of Φ is the value calculated by Tscheogl[27] with $\epsilon = 0.2$. This agrees roughly with the present results though $\langle r^2 \rangle = 6\langle s^2 \rangle$ does not hold exactly in a good solvent. However, if we draw a best fit line for all the data points, the slope is 0.33, somewhat higher than the expected slope. We consider that this difference might be due to the ambiguity of approximately 20% in estimating $\Delta\epsilon$ as discussed above.

Acknowledgment. This work was supported in part by the Grant-in-Aid for Scientific Research by the Ministry of Education, Science and Culture (C6055062, 1985–1986). Support from the Institute of Polymer Research, Osaka University, is also gratefully acknowledged.

Registry No. PI, 9003-31-0.

References and Notes

(1) Stockmayer, W. H. *Pure Appl. Chem.* **1967**, *15*, 539.
(2) North, A. M. *Chem. Soc. Rev.* **1972**, *1*, 49.
(3) Block, H. *Adv. Polym. Sci.* **1979**, *33*, 93.
(4) Stockmayer, W. H.; Baur, M. E. *J. Am. Chem. Soc.* **1964**, *86*, 3485.
(5) Baur, M. E.; Stockmayer, W. H. *J. Chem. Phys.* **1965**, *43*, 4319.
(6) Stockmayer, W. H.; Burke, J. J. *Macromolecules* **1969**, *2*, 647.
(7) Jones, A. A.; Stockmayer, W. H.; Molinari, R. J. *J. Polym. Sci., Polym. Symp.* **1976**, *54*, 227.
(8) Mashimo, S.; Yagihara, S.; Chiba, A. *Macromolecules* **1984**, *17*, 630.
(9) Adachi, K.; Kotaka, T. *Macromolecules* **1983**, *16*, 1936.
(10) Adachi, K.; Kotaka, T. *Macromolecules* **1984**, *17*, 120.
(11) Adachi, K.; Kotaka, T. *Macromolecules* **1985**, *18*, 294.
(12) Adachi, K.; Kotaka, T. *Macromolecules* **1985**, *18*, 466.
(13) Adachi, K.; Okazaki, H.; Kotaka, T. *Macromolecules* **1985**, *18*, 1486.
(14) Adachi, K.; Okazaki, H.; Kotaka, T. *Macromolecules* **1985**, *18*, 1687.
(15) Adachi, K.; Kotaka, T. *Polym. J.* **1986**, *18*, 315.
(16) Adachi, K.; Ohta, K.; Kotaka, T. *Polym. J.* **1986**, *18*, 371.
(17) Bates, T. W.; Ivin, K. J.; Williams, G. *Trans. Faraday Soc.* **1967**, *63*, 1964.
(18) Rouse, P. E. *J. Chem. Phys.* **1953**, *21*, 1272.
(19) Zimm, B. H. *J. Chem. Phys.* **1956**, *24*, 269.
(20) Muthukumar, M. *Macromolecules* **1984**, *17*, 971.
(21) Muthukumar, M.; Freed, K. F. *Macromolecules* **1978**, *11*, 843.
(22) Böttcher, C. J. F. *Theory of Electric Polarization*; Elsevier: Amsterdam, 1973; Vol. 1.
(23) Poddubnyi, I. Y.; Ehrenberg, E. G. *J. Polym. Sci.* **1962**, *57*, 545.
(24) Lodge, T. P.; Miller, J. W.; Schrag, J. L. *J. Polym. Sci., Polym. Phys. Ed.* **1982**, *20*, 1409.
(25) Ferry, J. D. *Viscoelastic Properties of Polymers*; Wiley: New York, 1961.
(26) *Polymer Hand Book*, 2nd ed.; Brandrup, J., Immergut, E. H., Eds.; Wiley: New York, 1975.

(27) Tschoegl, N. W. *J. Chem. Phys.* **1964**, *40*, 473.
(28) Ptisyn, O. B.; Eizner, Yu. E. *Zh. Fiz. Khim.* **1958**, *32*, 2464.
(29) Zimm, B. H.; Roe, G. L.; Epstein, L. F. *J. Chem. Phys.* **1956**, *24*, 279.
(30) Verdier, P. H. *J. Chem. Phys.* **1973**, *59*, 6119.
(31) Dial, M.; Crabb, K. S.; Crabb, C. C.; Kovac, J. *Macromolecules* **1985**, *18*, 2215.
(32) Flory, P. J.; Fox, T. G. *J. Am. Chem. Soc.* **1951**, *73*, 1907.

Use of the Pariser–Parr–Pople Approximation To Obtain Practically Useful Predictions for Electronic Spectral Properties of Conducting Polymers

Paul M. Lahti,*† Jan Obrzut,‡ and Frank E. Karasz‡

Departments of Chemistry and of Polymer Science and Engineering, University of Massachusetts, Amherst, Massachusetts 01003. *Received August 15, 1986*

ABSTRACT: Use of a Pariser–Parr–Pople model for estimating band gaps (E_g) for several potentially conducting conjugated polymers of recent interest gives good correlation with experimental values by extrapolation of computed E_g values as a function of reciprocal chain length of model oligomers. Hydrocarbon polymers of 1,3-phenylene, 1,4-phenylene, 1,4-phenylenevinylene, perinaphthalene, and related monomers seem well modeled by this method, as well as polymers of heterosubstituted conjugated monomers such as 2,5-pyrrole, 2,5-thiophene, 2,5-thiophendiylvinylene, and related species. The method should be useful as an inexpensive best first approximation to the band gaps of putative conjugated polymers and hence of interest to synthetic polymer chemists interested in such molecules.

Predictive computational chemistry can play an important role in the rapidly growing field of conducting doped polymers,[1-7] if it can help systematically to identify polymers that are most likely to have desirable electronic properties. We find that use of a variation of the well-known Pariser–Parr–Pople (PPP) semiempirical model for predicting electronic excited-state transition energies leads to predictions for long-wavelength excitation energies—i.e., band gaps, E_g—that are generally in good agreement with experimental results to date. Since the PPP method is highly approximate, it cannot hope to substitute for the hypothetical rigor of higher level, more expensive computational prediction, but we feel that the results obtained at negligible expense show the usefulness of the model as a practical method for finding electronic transition energies for conjugated molecules, where more precise methods are unavailable or economically impractical.

Various methods have been used to study the electronic nature of conducting polymers, ranging from Hückel-type models[8] to CNDO-S2[9] and MNDO[10-11] semiempirical methods. Use of ab initio methods in such cases is prohibitively expensive for any but the simplest model system. Recently, Brêdas[12-16] adapted the valence-effective Hamiltonian (VEH) method of Nicolas and Durand[17] for application to electronic properties of polymer and achieved a good practical degree of success in modeling polymer electronic properties, using geometries obtained by other methods. The VEH method was designed for prediction of valence band properties and has proved successful in this role. Although the theoretical basis for the success of the VEH model in application to optical spectroscopy is less clear,[12] VEH is one of the more successful—though not yet widely available—methods of obtaining useful predictive information concerning electronic properties of polymers.

The Pariser–Parr–Pople (PPP) model[19,20] is well adapted for obtaining π-symmetry electronic transitions for conjugated systems, and though it has a number of notable limitations[19-21] it has the advantages of wide availability, computational parasimony, and a good record of success in predicting π-type transition energies and intensities.[21-25] We used the Hinze–Beveridge PPP model with configuration interaction (PPP–CI) model to obtain spectral transition energies and intensities for oligomers of increasing chain length in a number of conjugated model systems and then applied the experimentally well-known[9,26-28] reciprocal rule for polymers, which states that many properties of homopolymers tend to vary linearly as functions of reciprocal chain length. For all computations, the parameters and algorithms are those given by the original workers[21] and will not be further described herein. Geometries for the oligomers used were obtained by extrapolation from known or similar cases or by comparison to monomer geometric parameters. In general, geometric changes of $\sim$0.04 Å in bond lengths or 5° in bond angles gave only small changes in the spectra predicted, as expected[14] for cases where small geometric changes do not actually change the basic repeat unit symmetry of the oligomer.

Table I shows PPP–CI long-wavelength transition energies and intensities for a variety of oligomeric species, with comparative experimental data. The agreement is good (as in PPP studies of other types of molecules[21-25]) considering that the PPP prediction corresponds to the energy of a putative gas phase 0–0 vertical transition without accounting for any macroscopic effects (e.g., solvent effects). Even in good solution phase studies, UV–vis bands tend to be broad and featureless, whereas polymer spectra must often be obtained on solid films or by reflectance, with attendant broadening and signal–noise problems. In most of the case studies, a long-wavelength transition with large oscillator strength (>0.7) was obtained, implying a strong transition. In a few cases a longer wavelength band of weak intensity was predicted, so the more intense transition was taken as representing the band gap, while the lower intensity band was taken as being part of the long-tailing absorption to low energy that is observed in many such cases. Table I thus enumerates the most intense long-wavelength bands (as well as predicted and experimental ionization potential data[29]) for various oligomeric species. Good agreement is found between predicted and observed E_g values for oligomeric conjugated species, thus encouraging extrapolation by the reciprocal

† Department of Chemistry.
‡ Department of Polymer Science and Engineering.

0024-9297/87/2220-2023$01.50/0